This article has been accepted for publication in a future issue of this journal, but has not been fully edited. Content may change prior to final publication. Citation information: DOI 10.1109/LAWP.2015.2464680, IEEE Antennas and Wireless Propagation Letters

Signal processing techniques for chipless UWB RFID thermal threshold detector detection

A. Lazaro, *Member, IEEE,* A. Ramos, *Student Member, IEEE,* D. Girbau, *Senior Member, IEEE,* and R. Villarino

***Abstract*—This paper presents signal processing techniques to detect a passive thermal threshold detector based on a chipless time-domain ultra-wideband (UWB) radio-frequency identification (RFID) tag. The tag is composed by a UWB antenna connected to a transmission line, in turn loaded with a biomorphic thermal switch. The working principle consists of detecting the impedance change of the thermal switch. This change occurs when the temperature exceeds a threshold. A UWB radar is used as the reader. The difference between the actual time sample and a reference signal obtained from the averaging of previous samples is used to determine the switch transition and to mitigate the interferences derived from clutter reflections. A gain compensation function is applied to equalize the attenuation due to propagation loss. An improved method based on the Continuous Wavelet Transform with Morlet wavelet is used to overcome detection problems associated to a low signal-to-noise ratio at the receiver. The average delay profile is used to detect the tag delay. Experimental measurements up to 5 m are obtained.**

***Index Terms*— Temperature sensor, Continuous Wavelet Transform (CWT), radio frequency identification (RFID), ultra-wideband (UWB), chipless**

I. Introduction

PASSIVE Radiofrequency Identification (RFID) systems have experienced tremendous growth in recent years [1-6].

Although passive RFID tags are oriented to item identification, potential applications of passive RFID technology require increasing its functionality by adding sensing capability to the tags. These could be used to sense different environmental conditions, i.e. temperature and humidity. Passive or semi-passive tags are thus a preferred option for low-cost sensor applications [1]. Consequently, during last years there has been a great interest in developing passive UHF RFID sensors. These tags are often based on detuning the antenna behavior by the sensor [1-3]. Alternatively, ultra-wideband (UWB) chipless tags for RFID systems might be a good alternative for low-cost item tagging, as recently demonstrated in [4-5]. Sensing functionalities have been considered in UWB tags. For example, passive temperature sensors based on the modulation of a UWB antenna have been reported in [6]. However, for some applications (i.e., alarms), a simple temperature threshold detector is sufficient, and potentially a lower cost solution. Thermal threshold sensors based on passive UHF RFID which use shape-memory alloys [2] or commercial thermal switches [3] can be found in the literature.

In this work, we report several techniques to make chipless UWB RFID systems detection more reliable, which are demonstrated when applied to a thermal threshold detector. The influence of some drawbacks associated to these systems, such as transmitter coupling, clutter interference, noise and interference from other wireless systems are addressed and improved using the proposed techniques. The detector is designed using a chipless time-coded UWB tag loaded with a commercial thermal switch. When the temperature exceeds a certain threshold, the impedance of the thermal switch changes. This change produces a modulation on the amplitude of the backscattered pulse in time-domain. An experimental setup based on a UWB radar working as a reader is proposed to measure the tag in time domain. A key point is the utilization of a differential detector to detect the change transition in the switch and to mitigate the interferences from the clutter reflections without the need to use background subtraction as in previous works [5-6]. In order to overcome detection problems at the receiver (associated to a low signal-to-noise ratio when the sensor-reader distance increases) a method based on the Continuous Wavelet Transform (CWT) which improves the one presented by the authors in [5] is used. In addition, a gain compensation function which is applied to equalize the attenuation due to propagation loss is also proposed. Moreover, the delay profile distribution is introduced to determine the range of the tag. Finally, strategies for tag detection are discussed.

The paper is organized as follows. Section II describes both the UWB system and the signal processing methods used to detect the tag, which are: the use of a differential coding schema and the improved CWT as matched filter. Section III presents the tag design and the experimental results. Finally, Section IV draws the conclusions.

II. System operation and signal processing

Fig. 1 shows the proposed system. It consists of a bistatic UWB radar that illuminates the tag. When the transmitted pulse hits the tag antenna, a portion of the pulse is backscattered towards the receiver, and another portion is propagated inside the tag. The backscattered field can be expressed as the sum of a structural and an antenna (or tag) mode [5]. The structural mode is the scattering originated due to the antenna shape, material and size; and it is independent

Manuscript received November 22, 2014. This work was supported by the Spanish Government Project TEC2011-28357-C02-01, H2020 Grant Agreement 645771–EMERGENT and an AGAUR Grant FI-DGR 2012.

The authors are with the Department of Electronic, Electric and Automatic Control Engineering, Universitat Rovira i Virgili, 43007 Tarragona, Spain. (e-mail: antonioramon.lazaro@urv.cat).

This article has been accepted for publication in a future issue of this journal, but has not been fully edited. Content may change prior to final publication. Citation information: DOI 10.1109/LAWP.2015.2464680, IEEE Antennas and Wireless Propagation Letters

of the fact that the antenna was specifically designed to transmit or receive RF signals. The tag (or antenna) mode is the portion of the energy captured by the antenna that is reradiated. This mode depends on the circuit connected to the antenna.

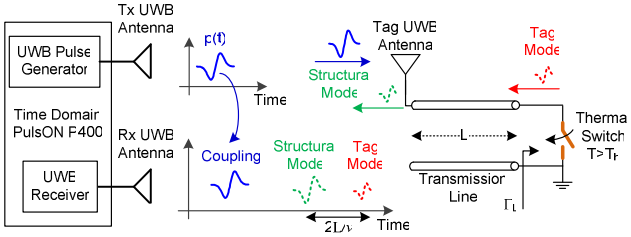

Fig. 1. System block diagram including the UWB radar reader and the sensor.

The backscattering field can be modeled using the circuit analogy described in [5] where the antenna is modeled using a two-port scattering matrix. Assuming that the RFID reader transmits a pulse $p(t)$, the signal $s(t)$ received at the reader can be expressed as [5]:

$$s(t) \approx \alpha\Gamma_{in}(t) * p(t) * \delta(t-\tau_p) = \alpha \cdot p_{sm}(t) * \delta(t-\tau_p) + \alpha \cdot p_{am}(t) * \Gamma_L(t) * \delta(t-\tau_p-\tau_L) \quad (1)$$

where * denotes the convolution operator, $p_{sm}(t)$ is the structural mode, $p_{am}(t)$ is the tag mode reflection pulse, and $\Gamma_L(t)$ is the inverse Fourier transform of the load reflection coefficient at the end of the transmission line. The time delay due to the propagation between the reader and the tag is denoted by τ_p. α is the attenuation due to the propagation, and $\tau_L=2L/v$ is the round-trip propagation delay along the transmission line, (where v is the propagation velocity in the transmission line). The delay τ_L can be used to identify one sensor from another [5]. Unfortunately, the radar receives undesired signals from other object reflections in the scene (clutter), and from the finite isolation between the transmitter and receiver (coupling). The coupling signal can be easily eliminated by gating the received signal in the time domain. This is because the separation between the reader's transmitting to receiving antennas is smaller than the separation between them and the tag.

The signal processing techniques used to detect the temperature state are summarized in Fig. 2. In order to reduce the effect of non-modulated clutter, the differential signal between two acquisitions is considered:

$$s_{dif}(t) \simeq s(t) - s_{ref}(t) = \alpha\, p_{am}(t) * \delta(t-\tau_P-\tau_L) * \Delta\Gamma_L(t) \quad (2)$$

where $\Delta\Gamma_L(t)$ is the differential reflection coefficient between two acquisitions, $s(t)$ and $s_{ref}(t)$. If the switch temperature does not change, $\Delta\Gamma_L = 0$. On the contrary, if the threshold is surpassed, $|\Delta\Gamma_L| = |\Gamma_{ON}-\Gamma_{OFF}|$. For both cases, the structural mode is suppressed, since it does not change between two different acquisitions. In practice, the reference signal can be obtained as the output of a moving averaging filter in order to reduce noise.

Signals at higher distances (long delays) have smaller amplitudes than those from closer distances (short delays). Therefore, it is needed to equalize amplitudes applying a time gain function, to compensate the attenuation due to the propagation loss [α in (1)]. α assumes that line-of-sight (LOS) propagation is inversely proportional to the square of distance or time delay. A gain compensation proportional to the square of time delay has been applied in order to compensate α.

The next step is to detect the tag mode reflections. An approach based on Continuous Wavelet Transform (CWT) has been successfully applied to detect time-domain coded chipless tags [5]. The CWT of a given function $s(t)$ is defined as the convolution of the signal and the time-shifted and scaled wavelet. $S_W(a,\tau)$ is the wavelet coefficient at delay τ and scale a. The CWT can be interpreted as a matched filter to the received signal. The amplitude of the CWT is maximized when the received signal shape is equal to one of the mother functions for a given optimum scale a_m and delay τ_m [5]. If a mother family similar to the expected waveform pulse is chosen, the CWT coefficients are the output of a matched filter or correlator. Several wavelet families have been proposed in the literature, depending on the application. Therefore it is fundamental the wavelet selection in order to recollect the maximum energy of the received pulse. In previous works [5-6] an impulse UWB radar that transmits an approximated monocycle UWB pulse has been used. Therefore, a complex Gaussian wavelet is used. In this work, the Time Domain PulsON P400 MRM impulse radar is used as the reader. From the specifications of the radar manufacturer, the UWB pulse is generated by switching and filtering the output of an oscillator centered at the center frequency of the radar (about 4.3 GHz). The output filter in the transmitter joined with the antennas allows complying with the FCC UWB regulation mask. Therefore, here the Morlet wavelet mother family [7] is proposed. It is given by $\psi(t)$ and its Fourier transform (ω):

$$\psi(t) = \pi^{-1/4} e^{j\omega_0 t} e^{-t^2/2}; W(\omega) = \pi^{-1/4} H(\omega) e^{-(\omega-\omega_0)^2/2} \quad (3)$$

where $H(\omega)$ is the Heaviside step function. The convolution can be done in the Fourier domain as a product of the Fourier Transforms. Then, the CWT can be efficiently implemented by using the Inverse Fast Fourier Transform (IFFT) algorithm [7].

$$S_W(a,\tau) = \sqrt{a}\,\Im^{-1}\{S(\omega)W(a\omega)\} \quad (4)$$

where $S(\omega)$ is the Fourier transform of the signal $s(t)$. Fig. 3 shows the spectrum of the typical pulse obtained from the reflection on a large plate using the transmitting and receiving antennas. The spectrums of the Morlet and 3th order complex Gaussian wavelet that maximizes the CWT are shown. For comparison purposes, the FCC UWB regulation masks have been superposed. It is shown that the optimum Morlet wavelet recollects better the pulse energy than the complex Gaussian wavelet. Therefore, the Morlet wavelet is more suitable for this type of transmitted pulses. The parameter ω_0 in the Morlet wavelet is chosen equal to the central frequency of the spectrum of the radar. Then, the optimum scale a_m adjusts the bandwidth of the wavelet. The value of a_m is practically unchanged between acquisitions. Therefore, the CWT is only computed for $a = a_m$. This reduces the number of Fourier transforms, saves computational time and permits a nearly real-time processing. Seeing the CWT as a frequency filter, the other major improvement by choosing the Morlet wavelet instead of the complex Gaussian wavelet is the greater

This article has been accepted for publication in a future issue of this journal, but has not been fully edited. Content may change prior to final publication. Citation information: DOI 10.1109/LAWP.2015.2464680, IEEE Antennas and Wireless Propagation Letters

rejection to interference signals from other wireless systems (such as mobile or ISM).

The next step is to decide a threshold for the temperature state estimation. To this end, the CWT coefficients for the maximum scale (a_m) are recorded in a matrix R_{mn}, where the row index m represents the number of radar acquisition and column index n represents the time delay of the acquired signal. Then, the average delay profile (APD) is computed as the average of the amplitudes for each row:

$$P(n) = (1/N)\sum_{m=1}^{N} |R_{mn}|^2 \quad (5)$$

The threshold is obtained by analyzing the column index n that maximizes the delay profile. It will be described with an example in Section IV.

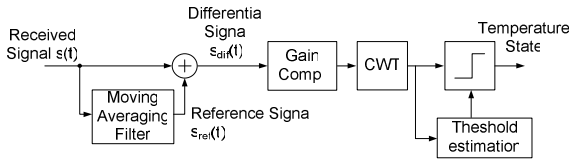

Fig. 2. Block diagram of the signal processing techniques.

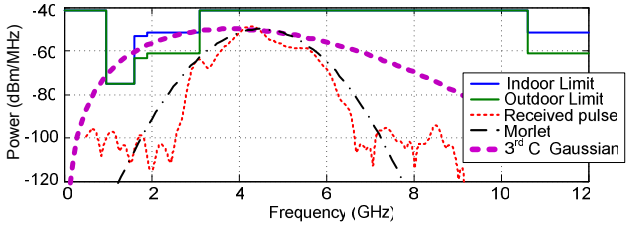

Fig. 3. Spectrum of received pulse, the 3th complex Gaussian and Morlet wavelets that maximize the CWT and the FCC indoor and outdoor limit masks.

III. TAG DESIGN AND MEASUREMENT RESULTS

A photograph of the tag is shown in Fig. 4. The tag is manufactured on Rogers RO4003C substrate. The tag is composed by a Vivaldi antenna with a slot to microstrip line transition, connected to a delay microstrip line. The Vivaldi antenna is characterized by its high bandwidth and moderated gain [6] compared with other UWB antennas such as fat monopoles. The delay is necessary to separate the structural and tag modes in time domain. It is also used to identify the tag. At the end of the line, a commercial threshold thermal switch model AIRPAX 67F050 is connected. From the manufacturer specifications, a 67F050 thermostat will close (make contact) when temperature surpasses the threshold of 50 ± 5 ºC. The antenna is approximately well matched (return loss lower than -10 dB) from 2 to 11 GHz. The thermal switch is characterized to verify its operation in the radar band (3.1 to 5.6 GHz). To this end, the switch is connected to a short microstrip line and to a PCB SMA connector. The input reflection coefficient of the switch is shown in Fig. 4 after the connector is deembedded. When the switch is cold (temperature below the threshold), it can be modeled as an open circuit. When it is hot (temperature above the threshold), the two arms of the switch are connected, behaving as a short circuit. At frequencies higher than 5 GHz the difference between the two states is smaller due to the parasitic effects. Although the switch is not designed to operate at high frequencies, it still works near the radar band. To evaluate the behavior of the switch, the ratio between the energy of the actual differential signal, and the maximum energy when the states difference are maximum $|\Delta\Gamma_L|=2$ (e.g. between ideal short and open circuit) is defined. It is the time domain modulation efficiency that can be computed in the frequency domain using the Parseval's theorem:

$$\eta_{\text{mod}} = \int_{-\infty}^{+\infty} |P_{am}(f)\Delta\Gamma_L(f)|^2 \, df \Big/ \int_{-\infty}^{+\infty} |2P_{am}(f)|^2 \, df \quad (6)$$

Where $P_{am}(f)$ is the Fourier transform of $p_{am}(t)$. It is found that η_{mod} = 18% for the switch states (from Fig. 4). η_{mod} can be improved by increasing the reflection coefficient $\Delta\Gamma_L$ in the centre frequency of the radar.

The time-domain response of the tag is characterized as a function of the temperature by heating the switch with a heat gun. In order to measure its temperature, a Positive Temperature Sensor (PTS) is placed on its dissipator and its resistance is measured using a multimeter. Several acquisitions have been performed at a distance of 50 cm between the tag and the reader. The signal coupled between transmitter and receiver antennas at the reader is removed by time gating, i.e., by selecting the start delay of the acquisition window of the radar. Fig. 5 shows the output of the CWT detector as a function of both the radar time delay and the PTS temperature for cold to hot state transition Fig.5(a) and vice versa Fig.5(b). A hysteresis in the threshold temperature between the two transitions is observed. This agrees with the switch's manufacturer specifications.

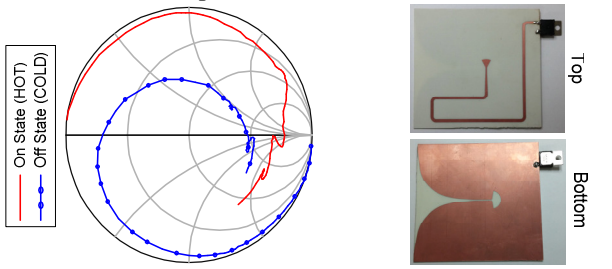

Fig. 4. (Left) Measured reflection coefficient for the two states (On and Off) of the switch between 10 MHz and 6 GHz. (Right) Photographs of the designed tag (top and bottom) Tag size: 83.43 x 78.4 mm^2.

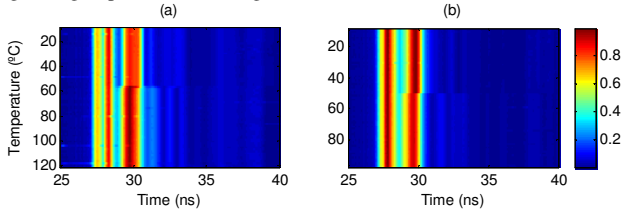

Fig. 5. Amplitude of the CWT as a function of the time delay and temperature. (a) Cold-to-hot state transition, (b) Hot-to-cold state transition.

Fig. 6 compares the amplitude at the output of the CWT detector for some acquisitions as a function of the time delay. The case of the transmission line loaded with an open circuit is also shown. The background (measurement of the scene without the tag) has been removed to reduce the clutter. For all the acquisitions it is observed that the structural mode remains constant. The tag mode depends on the reflection at the end of line, which is loaded by the switch. The structural mode of the Vivaldi antenna when it is well oriented is lower than the tag mode. The tag mode changes when the temperature reaches

This article has been accepted for publication in a future issue of this journal, but has not been fully edited. Content may change prior to final publication. Citation information: DOI 10.1109/LAWP.2015.2464680, IEEE Antennas and Wireless Propagation Letters

the threshold (about > 50 ºC). The threshold temperature is within the typical values given by the switch manufacturer (50 ± 5 ºC). The threshold can be adjusted by changing the model of the switch within the product series in steps of 10 ºC from 40 to 100 ºC. Fig. 6 demonstrates that it is possible to determine the switch state by using a simple level comparator at the output of the CWT. In order to study the read range of the sensor, measurements at different distances have been performed. Fig.7 shows results at a distance of 5 m between the tag and the reader. Initially the tag is heated up to a temperature higher than the threshold temperature (hot state). Then, several acquisitions have been measured while the temperature of the tag decreases. Fig. 7a shows the maximum of the CWT for different acquisitions after background subtraction is applied (measurement without the tag). Fig. 7b shows the maximum of the CWT after the gain compensation has been applied. Finally, undesired clutter is removed using $s_{ref}(t)$, avoiding the use of the background subtraction technique [5-6]. This reference signal is obtained by averaging the first acquisitions. This is feasible because the switch state is known when monitoring starts, and before the temperature could exceed the threshold. Hence, the differential signal (Fig. 7c) is obtained using the procedure described in Fig.2 by subtracting each acquisition from the reference signal (2). The temperature state is obtained by comparing the output of CWT with a threshold value. Fig. 8 shows the average delay profile distribution (6) of the CWT, obtained from the averaging of all acquisitions for each time delay. The peak corresponds to the maximum variation of the differential signal due to the change in the antenna mode of the sensor. From the time delay of the peak, it is easy to localize the tag distance. A cut of the output of CWT for this time delay is shown in Fig. 8b. Fig. 8c shows the complementary distribution function of the amplitudes of Fig. 8b. According this function, the threshold is fixed to the midpoint between the minimum and the maximum points. The measurements whose amplitude is higher than this threshold value corresponds to hot switch states. In addition, the fraction of time when the detector is cold (T_{COLD}/T) can be obtained from this graphic.

IV. Conclusion

This work has presented a set of signal processing techniques to detect chipless UWB time-domain sensors. These techniques have been applied to measure the change of impedance of a novel passive thermal threshold switch using a commercial bimetallic thermostat. In order to avoid the practical drawbacks of background subtraction techniques, a differential detector is proposed to detect the change transition and to mitigate the interferences that come from clutter reflections. In addition, a gain compensation function is applied to reduce the clutter amplitude due to reflections at nearby objects. The Continuous Wavelet Transform is used in order to overcome detection problems associated to a low signal-to-noise ratio at the receiver when the tag-reader distance increases. The selection of the wave mother function has been discussed in order to capture the maximum pulse energy and increases the signal-to-noise ratio. The results show that it is possible to remotely detect the temperature state of the switch up to 5 m in an indoor environment.

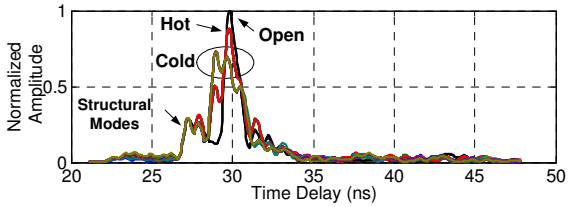

Fig. 6. Normalized amplitude of the CWT from the optimum scale as a function of the time delay for hot and cold states and open ended case.

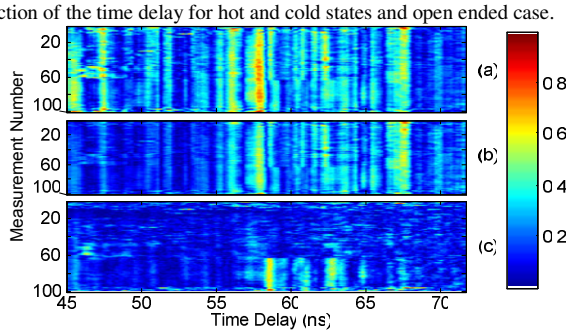

Fig. 7. Normalized amplitude of the CWT for the optimum scale before (a) and after (b) applying gain compensation. (c) Normalized amplitude of the CWT of the Differential signal. The distance between reader and tag is 5 m.

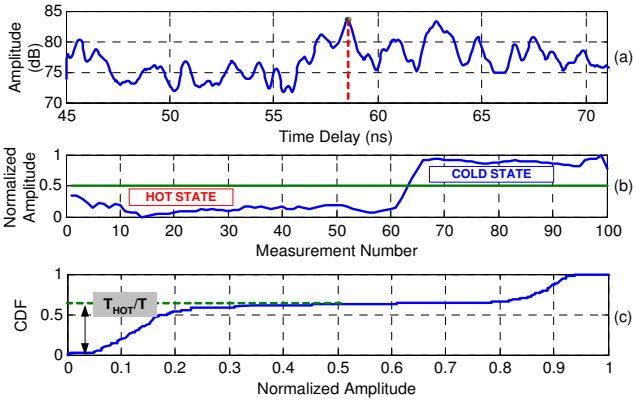

Fig. 8 (a) Average delay profile distribution (ADP) of the CWT results. (b) Normalized amplitude for the delay of the peak of ADP and threshold value used in the state decision. (c) CDF plot.

References

[1] G. Marrocco and F. Amato, "Self-sensing passive RFID: From theory to tag design and experimentation," *Microwave Conference EuMC 2009*, pp.1-4, 2009.

[2] S. Caizzone, C. Occhiuzzi, and G. Marrocco, "Multi-Chip RFID Antenna Integrating Shape-Memory Alloys for Detection of Thermal Thresholds," *IEEE Transactions On Antennas and Propagation*, Vol 59, No. 7, pp. 2488-2494, 2011.

[3] Z. Jiang and F. Yang, "Reconfigurable Sensing Antennas Integrated With Thermal Switches for Wireless Temperature Monitoring", *IEEE Antennas and Wireless Propagation Letters*, Vol. 12, pp. 914-917, 2013.

[4] S. Preradovic, I. Balbin, N. Chandra Karmakar, and G. F. Swiegers, "Multiresonator-Based Chipless RFID System for Low-Cost Item Tracking", *IEEE Transactions On Microwave Theory and Techniques*, Vol. 57, No 5, pp. 1411-1419, 2009.

[5] A. Lazaro, A. Ramos, D. Girbau, and R. Villarino, "Chipless UWB RFID Tag Detection Using Continuous Wavelet Transform," *IEEE Antennas and Wireless Propagation Letters*, Vol. 10, pp. 520-523, 2011.

[6] D. Girbau, A. Ramos, A. Lazaro, S. Rima, and R. Villarino, "Passive wireless temperature sensor based on time-coded UWB chipless RFID tags," *IEEE Transactions on Microwave Theory and Tech.*, Vol. 60, No. 11, pp. 3623-3632, 2012.

[7] S. Mallat, "A Wavelet Tour of Signal Processing," *Elsevier*, Burlington, MA, USA, 2009. ISBN 978-0-12-374370-1.